SAKARYA ÜNİVERSİTESİ FEN BİLİMLERİ ENSTİTÜSÜ DERGİSİ
SAKARYA UNIVERSITY JOURNAL OF SCIENCE

e-ISSN: 2147-835X
Dergi sayfası: http://dergipark.gov.tr/saufenbilder

Geliş/Received
08-09-2017
Kabul/Accepted
19-06-2017

Doi
10.16984/saufenbilder.337279

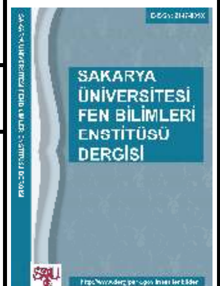

Evaluation of the pre-irradiation electrical characteristics of the RadFET dosimeters with diverse gate oxides by TCAD simulation program

Ayşegül Kahraman*[1] , Ercan Yılmaz[2]

ABSTRACT

The aim of the present study is to determine the pre-irradiation threshold voltages of the RadFET dosimeters with gate oxide composed of high-k dielectrics and compare the results with the traditional sensors, the gate oxide of which is composed of SiO_2. The effects of the p^+ regions with different concentration, depth and length on the electrical characteristic of the RadFETs were also investigated in the study. For these purposes, Al_2O_3, HfO_2 high-k dielectrics and SiO_2 with the thicknesses of 400 nm were used as the sensitive regions of the dosimeters. The sensors were designed in the Silvaco TCAD simulation program. While the lengths of the p^+ regions changed the I_d-V_g characteristics of the RADFETs, the depths and concentrations until a certain value of these regions did not play an important role in electrical characteristic. The lowest threshold voltages obtained from the SiO_2, Al_2O_3 and HfO_2-RadFETs were found to be -5.22, -3.63, and -3.10 V, respectively. These results demonstrated that RadFETs with high-k dielectrics may be promising candidate for the new generated dosimeters in terms of broader measurable dose range providing their radiation tests.

Keywords: RadFET, TCAD, high-k, threshold voltage

Farklı kapı oksitli RadFET dozimetrelerinin ışınlama öncesi elektriksel karakteristiklerinin TCAD benzetim programı ile değerlendirilmesi

ÖZ

Bu çalışmanın amacı, kapı oksiti yüksek-k'lı dielektriklerden oluşan RadFET dozimetrelerinin ışınlama öncesi eşik gerilimlerini belirlemek ve sonuçları, kapı oksiti SiO_2'den oluşan geleneksel sensörlerle kıyaslamaktır. Ayrıca çalışmada, farklı konsantrasyonlu, derinlikli ve genişlikli p^+ bölgelerinin RadFET'lerin elektriksel karakteristiği üzerine etkileri de incelenmiştir. Bu amaçla, dozimetrelerin duyar bölgeleri olarak 400 nm kalınlığında yüksek-k'lı Al_2O_3, HfO_2 dielektrikleri ve SiO_2 kullanılmıştır. Sensörler, Silvaco TCAD benzetim programında tasarlanmıştır. p^+ bölgelerinin uzunlukları, I_d-V_g karakteristiğini değiştirirken, bu bölgelerin derinlikleri ve belirli bir değere kadar konsantrasyonları elektriksel karakteristikte önemli bir rol oynamamıştır. SiO_2, Al_2O_3 ve HfO_2-RadFET'lerden elde edilen en düşük eşik voltajları sırasıyla, -5.22, -3.63 ve -3.10 V olarak bulunmuştur. Bu sonuçlar, yüksek-k

[1] Uludağ Üniversitesi Fen Edebiyat Fakültesi Fizik Bölümü, 16059, Nilüfer/BURSA-aysegulk@uludag.edu.tr
[2] Abant İzzet Baysal Üniversitesi Nükleer Radyasyon Dedektörleri Uygulama ve Araştırma Merkezi, 14280, BOLU-yilmaz@ibu.edu.tr

© 2017 Sakarya Üniversitesi Fen Bilimleri Enstitüsü

dielektrikli RadFET'lerin, radyasyon testlerinin yapılması koşuluyla, daha geniş ölçülebilir doz aralığı açısından yeni nesil dozimetreler için gelecek vaat eden bir aday olduğunu göstermektedir.

Anahtar Kelimeler: RadFET, TCAD, yüksek-k, eşik voltajı

1. INTRODUCTION

Radiation Sensing Field Effect Transistors (RadFETs), also known as pMOS transistor or p-MOSFET, has found many application areas such as radiotherapy, space radiation monitoring, high energy physics laboratories following the idea on its usability of ionizing radiation dosimeter or sensor reported by Holmes-Siedle [1-4]. The advantages of these dosimeters are: small size, excellent compatibility with CMOS technology, low power consumption, non-destructive and immediate read-out, wide dose range, etc. [5-6].

Radiation dosimeters are divided into two groups as active and passive dosimeters. TLDs are most commonly used in passive dosimeters. A great change is observed in the sensitivities of TLDs and their use is time consuming due to the complicated annealing mechanism and calibration process [7]. The use of diode detectors depends on dose rate and temperature [7]. However, the response of RadFETs is independent of dose rate up to 10^8 Gy/s and is less affected from temperature than diode's response [8-9].

The most important parameter affecting the sensitivity of the RadFET is gate oxide thickness. It is expected that the sensitivity/threshold voltage shift increases with increasing thickness of the gate oxide [10]. For instance, the RadFET with the gate oxide thickness of 100 nm (100 nm-RadFET) for 6 MV X-ray and 6 MeV electron beams obtained from LINAC (Linear Accelerator) showed lower sensitivity compared to 400 nm-RadFET [6]. However, deviation from the linearity is observed with increasing gate oxide thickness (~ 1 μm) in the lower dose range. Because, more oxide trapped charges occur due to increasing interaction probability of radiation with medium and this case leads to electric field screening [5-6]. Most of the commercial RadFETs have gate oxide thickness of 400 nm due to their linear performances for a wide dose range compared to pMOS with thicker gate oxide and higher sensitivity compared to RadFET with thin gate oxide [5, 11].

The literature studies on RadFET can be separated into a few groups: i) Investigation of the package lid effect on the sensitivity of the sensor [12-13], ii) Determination of the short and long term fading characteristics of pMOS transistor [5, 14], iii) The calculation of the trap densities for pre-irradiation and post-irradiation [15-16], iv) Investigation of the effects of different production parameters such as annealing, boron ion (B^+) implantation on the sensitivity of dosimeter [17]. However, most of the studies are based on RadFETs with SiO_2 (gate oxide/sensitive region) grown by wet-dry oxidation process. The studies on the RadFET with high-k dielectric are very few in the literature [12, 18-19]. The reason of the choice of the SiO_2 as gate dielectric is the perfect interface formation between the Si and SiO_2. The interface between the high-k and Si contains many structural defects due to the lattice mismatch and so, the interface traps increase. However, the post deposition annealing process improves the interface quality and it is possible to fabricate the RadFET with thinner gate oxide by high-k dielectrics due to the larger charge storage capacity of the high-k MOS structure compared to the device with SiO_2 [20-21]. On the other side, some experimental studies on the MOS capacitors having the oxide with high-k dielectric have shown that their responses to ^{60}Co gamma source are higher than traditional MOS capacitor with SiO_2 gate oxide [22-24]. There are also studies showing that MOS capacitors with different dielectrics are less sensitive to radiation compared to the structure with SiO_2 [25-26]. These results may also be valid for the pMOS transistor including the MOS structure. These findings are crucial in pointing out that RadFETs are sensors that can be designed for their intended use.

Low threshold voltage (V_{th}) for pre-irradiation is an important factor in terms of production of RadFET with broader measurable dose range and the studies on zero threshold voltage adjustment of SiO_2-RadFET have continued [11, 17]. Therefore, investigation of the electrical characteristics of the RadFETs with high-k dielectrics is quite important to determine the minimum pre-irradiation threshold voltages of different sensors.

The zero threshold voltage adjustment for SiO_2-RadFET is made by B^+ ion implantation to the gate

oxide (SiO_2) [11, 17]. Therefore, fabrication time/step is increasing with this process. However, RadFETs with high-k dielectrics have lower threshold voltages without ion implantation [27] and thus RadFETs with broader measurable dose range can be obtained. On the other hand, the investigation of the effect of the B^+ ion concentrations in p^+ regions on the electrical characteristics of RadFET is also very important for the evaluation of fabrication processes, because the variation in the concentration in these regions can affect the current and threshold voltages. For this reasons, the aims of the present study are: i) to investigate the electrical characteristics of RadFETs with different gate oxide layers and to determine the initial threshold voltages, ii) to examine the effect of B^+ ion concentration on the electrical characteristic of RadFET. In this context, the pre-irradiation threshold voltages of RadFETs with high-k dielectrics of HfO_2 (~25) [28] and Al_2O_3 (~9) [29] were investigated by Silvaco TCAD simulation program and the results were compared with the traditional RadFET with SiO_2 (~3.9) [29]. For all of the RadFETs, the effects of the depth, wide and concentrations of the p^+ regions on the current-voltage (I_d-V_g) characteristics of RadFETs were also determined. These results form the basis of further experimental works on RadFET with high-k dielectric. In this work, theoretical/simulation results for RadFETs are given.

2. THEORY AND STRUCTURE

The RadFET fabricated on n-type Si wafer has four terminals: source, gate, drain and bulk-silicon. Boron is used as p-type dopant for the p^+ regions in these transistors. The channel should be formed between the two p^+ regions for the current transition and number of charge carriers in the channel is controlled by the gate voltage. The events in the structure depending on the applied gate voltage (V_g) are: i) The negative charges in the Si move to channel with applied positive gate voltage (accumulation regime), ii) The depletion region occurs with the applied negative voltage (depletion regime), iii) By increasing the applied negative voltage, hole concentration exceeds the electron concentration in the channel or near oxide/Si interface (inversion regime). For the positive charge flows, V_g should be more negative than V_{th}. In this study, the intersection of the straight line obtained from linear region of I_d-V_g characteristic curve with voltage axis was taken as threshold voltage of RadFET [30].

The operation principle of the RadFET is based on the electron-hole pairs, occurring as a result of radiation interaction with sensitive region (gate oxide) of RadFET. Few of the electrons and holes recombine within a short time and most of them move under DC voltage. Electrons can easily escape from the traps due to their relatively higher mobility compared to holes. Due to their slow mobility, holes are trapped in the oxide layer or oxide/Si interface. The trapped charges cause the threshold voltage shift of the RadFET and post-irradiation V_{th} is more negative than before. The threshold voltage shifts corresponding to each applied dose are determined and these values constitute the calibration curve of the sensor. The schematic structure of the RadFET and radiation induced events are given in Figures 1a and 1b, respectively.

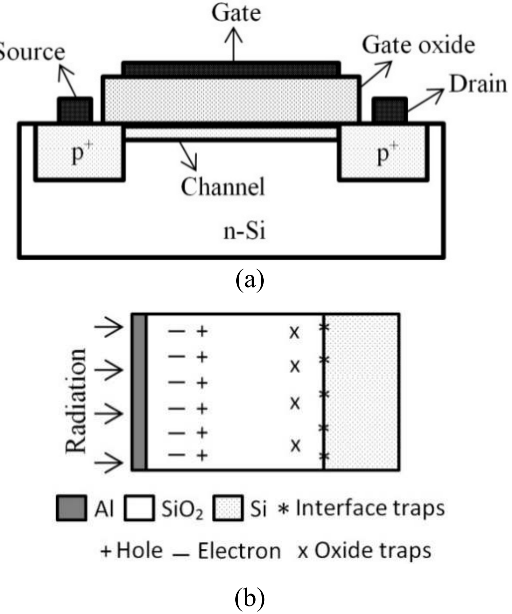

Figure 1. (a) Schematic view of the RadFET, (b) Radiation induced events in the sensor

The minimum detectable dose for SiO_2-RadFET is 1 cGy and the maximum dose is 1 kGy or higher, depending on the application requirements. There is more than one device in a single chip, and their channel width/length ratios are different. For electron and photon beams, the sensitivity of the sensor increases with decreasing channel length [6]. In the RadFET used in the simulation, the thickness of the Si layer and the channel width were selected as 500 µm and 15 µm, respectively. The length of the channel changed depending on the length of the p^+ regions.

Gaussian distribution was used for the B^+ implantation in the simulation and the concentration is expressed as [31]:

$$N(x) = \frac{\phi}{\sqrt{2\pi}\Delta R_p} exp\frac{-(x-R_p)^2}{2\Delta R_p{}^2} \quad (1)$$

Where N(x) is the B^+ concentration from the surface to x (µm) depth, $\emptyset$ is the B^+ ion dose, R_p is the projected range and ΔR_p is the standard deviation.

The threshold voltage of a p-type MOSFET (n-type substrate) is expressed as [32]:

$$V_{th} = V_{fb} - 2\emptyset_F - \frac{\sqrt{2\varepsilon_s q N_d (2\emptyset_F)}}{C_{ox}} \quad (2)$$

Where V_{fb} is the flat band voltage, $\emptyset_F$ is the Fermi potential, ε_s is the dielectric permittivity of Si, q is the electric charge, and N_d is the concentration of donor atoms.

The I_d current in RadFETs is given by [32]:

$$I_d = \frac{\mu W C_{ox}}{2L_{eff}}(V_g - V_{th})^2 \quad (3)$$

Where μ is the charge-carrier effective mobility, W is the gate width, L is the effective channel length.

3. SIMULATION PROCEDURE

Silvaco TCAD simulation program consists of ATHENA and ATLAS simulators. The DeckBuild Command Menu is used to create the input files and activates the sub-programs. ATHENA is used for the process (fabrication steps) simulation and ATLAS is a physically-based device simulator [31, 33]. The electrical characteristics (I_d-V_g) of the RadFETs were obtained from the ATLAS. The design steps of the RadFET in the ATLAS are: i) The Si and gate oxide (SiO_2, HfO_2, and Al_2O_3) with 400 nm thickness were defined to program as region 1 and region 2, respectively. ii) Gate, source, drain and substrate electrodes of the RadFET were determined on the structure. iii) Uniform n-type doping with 10^{15} atoms/cm^3 was applied to previously determined region of the Si (previously labelled as region 1 in the program). So, n-type Si was formed in the program. iv) p-type doping by Gaussian profile with different peak concentrations (10^{20}, 10^{19}, 10^{18}, and 10^{17} atoms/cm^3) was applied to form the p^+ regions of the RadFET. The junction and length data of the p^+ regions was externally defined to the program for Gaussian distribution. The view of minimized RadFET obtained from Tonyplot of TCAD is given in Figure 2.

4. RESULTS AND DISCUSSION

I_d-V_g characteristics of the RadFET with SiO_2 were obtained depending on different depths of the p^+ region with 10^{20} atoms/cm^3 and the results were given in the Figure 3. As shown in this figure, increasing depths of the p^+ regions did not lead to important variation on the I_d-V_g curves and no shifts in the threshold voltages of the SiO_2-RadFET were observed. This result is in compliance with the literatures [19, 32] since the drain current (I_d) depends on oxide capacitance, gate and threshold voltages, width and length of the gate/channel area.

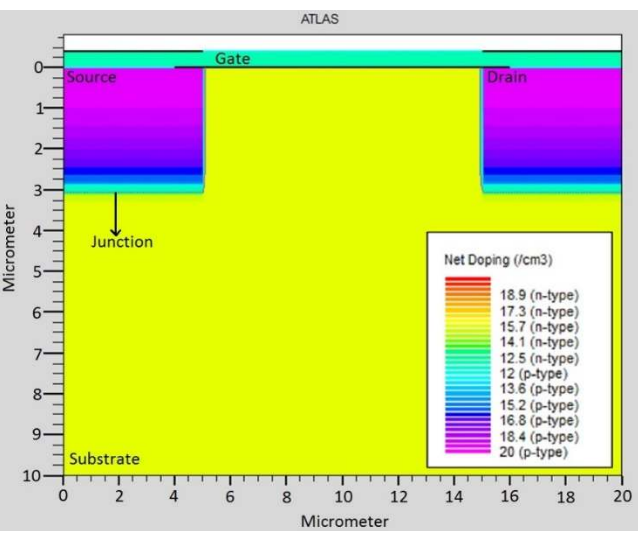

Figure 2. RadFET with the junction of 3 µm obtained from Tonyplot of TCAD (peak concentration of 10^{20} atoms/cm^3)

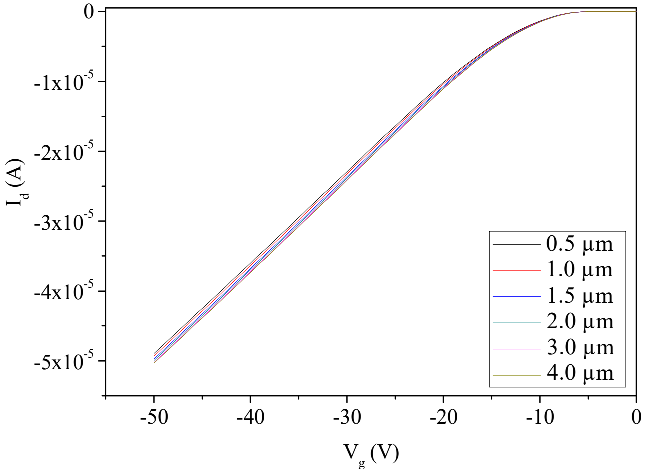

Figure 3. I_d-V_g characteristics of the SiO_2-RadFET with different junctions/depths of the p^+ regions

The I_d-V_g curves of the RadFETs with the gate oxides of SiO_2, Al_2O_3 and HfO_2 for different depth and width of the p^+ regions were presented in Figures 4, 5, and 6, respectively. It can be clearly seen from these figures that drain current increases with increasing dielectric constants (k) of the oxides. Because, the capacitance of the MOS structure depends on the dielectric constant of the gate oxide and the charge storage capacity is enhanced with increasing dielectric constant. On the other side, I_d changed with decreasing channel length or increasing p^+ region's lengths due to easy transportation of the charges from the source to the drain. The obtained results are in agreement with Eq. (3).

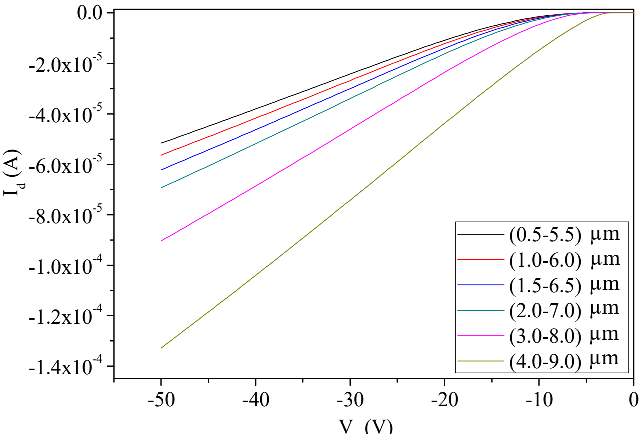

Figure 4. I_d-V_g characteristics of the SiO_2-RadFET with different depths and lengths of the p^+ regions

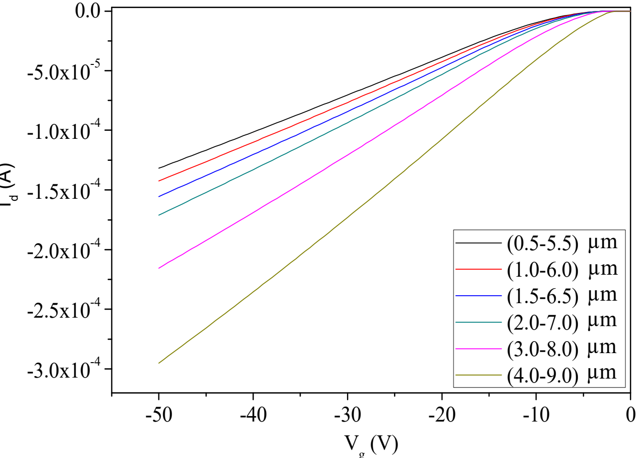

Figure 5. I_d-V_g characteristics of the Al_2O_3-RadFET with different depths and lengths of the p^+ regions

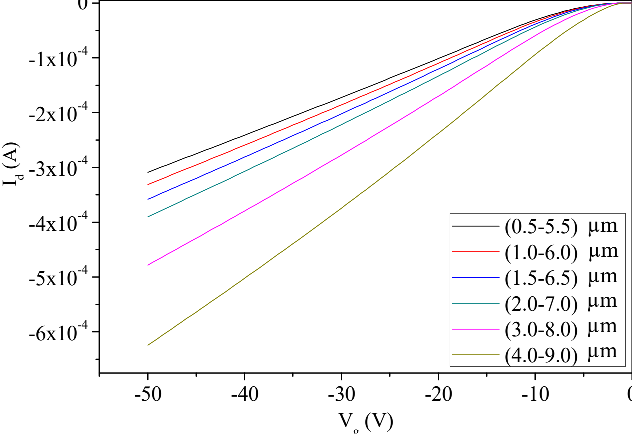

Figure 6. I_d-V_g characteristics of the HfO_2-RadFET with different depths and lengths of the p^+ regions

The threshold voltage results are presented in Table 1. These data demonstrated that the threshold voltage was getting closer to zero with increasing dielectric constant of the oxide. The oxide capacitance (C_{ox}) increases with increasing dielectric constant and the threshold voltage decreases as seen from Eq. (2). These results meet the theoretical expectation. The channel between the source and drain can be easily formed in the HfO_2-RadFET with the highest dielectric constant compared to others due to increasing charge storage capacity. Therefore, the threshold voltage shifts towards less negative values in the case of HfO_2-RadFET than others. The threshold voltages for the RadFETs with the gate oxides of SiO_2, Al_2O_3 and HfO_2 were found in the range of -8.96 – -11.59 V, -3.63 – -7.73 V, -3.10 – -5.98 V, respectively. The lowest V_{th} value was obtained as -3.10 V for HfO_2-RadFET with the 4.0 μm depth and 9.0 μm length of p^+ region. The highest V_{th} value was found to be -11.59 V for SiO_2-RadFET with the 0.5 μm depth and 5.5 μm length of p^+ region.

Table 1. Threshold voltages for different RadFETs

Sensor (k)	D-L (μm)	V_{th} (V)	Sensor (k)	D-L (μm)	V_{th} (V)
SiO_2-RadFET (~3.9)	0.5-5.5	-11.59	Al_2O_3-RadFET	2.0-7.0	-6.64
	1.0-6.0	-11.11		3.0-8.0	-5.68
	1.5-6.5	-10.76		4.0-9.0	-3.63
	2.0-7.0	-10.16	HfO_2-RadFET (~25)	0.5-5.5	-5.98
	3.0-8.0	-8.96		1.0-6.0	-5.36
	4.0-9.0	-5.22		1.5-6.5	-5.11
Al_2O_3-RadFET (~9)	0.5-5.5	-7.73		2.0-7.0	-5.01
	1.0-6.0	-7.26		3.0-8.0	-4.36
	1.5-6.5	-6.90		4.0-9.0	-3.10

The effect of p-type doping concentration on the I_d-V_g characteristic of the HfO_2-RadFETs was investigated and the results are given in Figure 7. No significant change was observed in the I_d-V_g curves with increasing p-type doping concentration except 10^{17} atoms/cm^3.

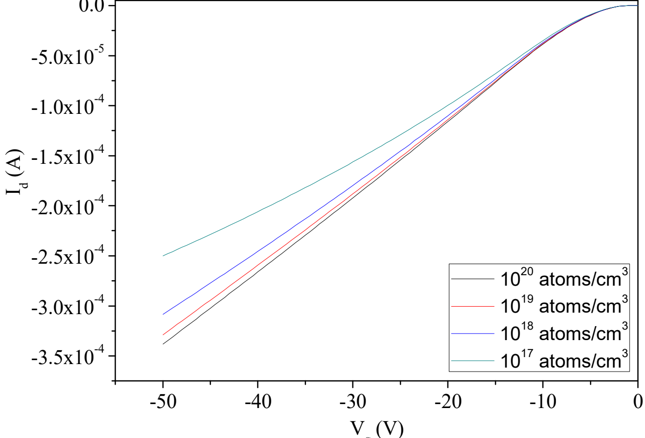

Figure 7. The I_d-V_g characteristic of the HfO_2-RadFET with different p-type doping concentration

5. CONCLUSION

In this work, the results of the pre-irradiation threshold voltages of the RadFET dosimeters with SiO_2, Al_2O_3 and HfO_2 gate oxides and the effect of the diverse depths/junctions and lengths of the p^+ regions of the sensor on the I_d-V_g characteristics were presented. The depth of the p^+ region of the SiO_2-RadFET was changed in the range of 0.5-4.0 μm and the electrical characteristic was investigated. The obtained results demonstrated that the depth of the p^+ regions did not change the I_d-V_g curves and threshold voltages. The V_{th} values were obtained from the I_d-V_g curves of the SiO_2, Al_2O_3 and HfO_2-RadFETs for the diverse depths and lengths of the p^+ regions. Threshold voltages were decreased with decreasing channel length due to easy transition of the charges between the source and drain. Increasing dielectric constant of the gate oxide also caused the threshold voltage to decrease due to higher charge storage capacity of the RadFET with high-k gate oxide compared to traditional sensor, the sensitive region of which is composed of SiO_2. In other words, The V_{th} value of the sensors was in descending order is: HfO_2-RadFET>Al_2O_3-RadFET>SiO_2-RadFET. The lowest V_{th} was obtained from the HfO_2-RadFET with 4.0 μm lengths and 9.0 μm depths as -3.10 V. The HfO_2-RadFETs with the different concentrations of the p^+ regions were designed for evaluation the effect of p^+ region's concentration on the electrical characteristic of the sensor. The results for the p-type doping concentrations varying from 10^{17}-10^{29} atoms/cm^3 demonstrated that the different concentrations did not lead to an important variation in the I_d-V_g characteristic of the HfO_2-RadFET except 10^{17} atom/cm^3. All of the results show that the RadFETs comprising of high-k dielectrics may play an important role for the dosimeter with broader measurable dose range. In RadFETs formed with high-k dielectrics, it is obvious that the threshold voltage is observed at lower values without applying any implantation process to the gate oxide layer compared to the structure with SiO_2. This is also very important in terms of shortening the production process. The I_d-V_g curves shift to greater negative voltages (shift to the left). Reduction in threshold voltage shift with radiation dose will extend the period of use of the sensor in high radiation dose environment such as space applications. On the other hand, it is essential to develop sensitivity to low doses for environmental measurements (greater shift of threshold voltage). The sensor can be designed to suit the application area with different high-k dielectrics. For these reasons, it is important to perform radiation tests of such sensors in future studies.

ACKNOWLEDGMENTS

This work is supported by The Scientific and Technological Research Council of Turkey (TÜBİTAK) 1002-Short Term R&D Funding Program under Contract Number: 114F260 and the Ministry of Development of Turkey under Contract Numbers: 2012 K 120360.

REFERENCES

[1] M.A. Carvajal, S. García-Pareja, D. Guirado, M. Vilches, M. Anguiano, A.J. Palma, A.M. Lallena, "Monte Carlo simulation using the PENELOPE code with an ant colony algorithm to study MOSFET

detectors," Phys. Med. Biol., vol. 54, pp. 6263-6276, Oct. 2009.

[2] J.O. Goldsten, R.H. Maurer, P.N. Peplowski, A.G. Holmes-Siedle, C.C. Herrmann, B.H. Mauk, "The engineering radiation monitor for the radiation belt storm probes mission," Space Sci. Rev., vol. 179, pp. 485-502, Nov. 2013.

[3] F. Ravotti, M. Glaser, A.B. Rosenfeld, M.L.F. Lerch, A.G. Holmes-Siedle, G. Sarrabayrouse, "Radiation monitoring in mixed environments at CERN: from the IRRAD6 facility to the LHC experiments," IEEE T. Nucl. Sci., Vol. 54, pp. 1170-1177, Aug. 2007.

[4] A. Holmes-Siedle, L. Adams, "RadFET-A review of the use of metal-oxide silicon devices as integrating dosimeters," Radiat. Phys. Chem., vol. 28, 235-244, 1986.

[5] G. Ristić, S. Golubović, M. Pejović, "Sensitivity and fading of pMOS dosimeters with thick gate oxide," Sensor. Actuat. A-Phys., vol. 51, pp. 153-158, Nov. 1995.

[6] M.S. Martínez-García, J. Torres del Río, A.J. Palma, A.M. Lallena, A. Jaksic, "Comparative study of MOSFET response to photon and electron beams in reference conditions," Sensor. Actuat. A-Phys., vol. 225, pp. 95-102, Apr. 2015.

[7] S.J. Cho, W.T. Kim, Y.G. Ki, S.I. Kwon, S.H. Lee, H.D. Huh, K.H. Cho, B.H. Kwon, D.W., Kim, "In Vivo Dosimetry with MOSFET Detector during Radiotherapy," IFMBE Proceedings, vol. 14/3, pp. 1987-1989, 2007.

[8] A.B. Rosenfeld, "Electronic dosimetry in radiation therapy," Radiat. Meas., pp. S134-S153, Dec. 2006.

[9] A. Holmes-Siedle, "Summary of REM's DOT Dosimeter System Based on the RadFET: Functionality, Stability and Applications. RADFET Probes, Readers, Applications". [Online]. Available: http://www.radfet.com/id4.html

[10] E. Yilmaz, İ. Doğan, R. Turan, "Use of Al_2O_3 layer as a dielectric in MOS based radiation sensors fabricated on a Si substrate," Nucl. Instrum. Meth. A, vol. 266, pp. 4896-4898, Nov. 2008.

[11] A. Jaksic, G. Ristic, M. Pejovic, A. Mohammadzadeh, W. Lane, "Characterisation of radiation response of 400 nm implanted gate oxide RADFETs," Proc. 23rd International Conference on Microelectronics (MIEL 2002), 2002, pp. 727-730.

[12] A. Kahraman, E. Yilmaz, S. Kaya, A. Aktag, "Effects of packaging materials on the sensitivity of RadFET with HfO_2 gate dielectric for electron and photon sources," Radiat. Eff. Defect. S., vol. 170, pp. 832-844, Oct. 2015.

[13] M. Wind, P. Beck, A. Jaksic, "Investigation of the energy response of RADFET for high energy photons, electrons, protons, and neutrons," IEEE T. Nucl. Sci., Vol. 56, pp. 3387-3392, Dec. 2009.

[14] A. Haran, A. Jakšić, N. Refaeli, A. Eliyahu, D. David, J. Barak, "Temperature effects and long term fading of implanted and unimplanted gate oxide RadFETs", IEEE T. Nucl. Sci., vol. 51, pp. 2917-2921, Oct. 2004.

[15] G.S. Ristíc, N.D. Vasović, M. Kovačević, A.B. Jakšić, "The sensitivity of 100 nm RADFETs with zero gate bias up to dose of 230 Gy(Si)," Nucl. Instrum. Meth. B, vol. 269, pp. 2703-2708, Dec. 2011.

[16] G.S. Ristíc, M. Andjelković, A.B. Jakšić, "The behavior of fixed and switching oxide traps of RADFETs during irradiation up to high absorbed doses," Appl. Radiat. Isotopes, vol. 102, pp. 29-34, Aug. 2015.

[17] S. Wang, P. Liu, J. Zhang, "Simulation of threshold voltage adjustment by B+ implantation for pMOS-RADFET application," Proc. 8th IEEE International Conference on Nano/Micro Engineered and Molecular Systems (NEMS), 2013, pp. 262-263.

[18] C. Andersson, C. Rossel, M. Sousa, D.J. Webb, C. Marchiori, D. Caimi, H. Siegwart, Y. Panayiotatos, A. Dimoulas, J. Fompeyrine, "Lanthanum germanate as dielectric for scaled germanium metal-oxide -semiconductor device," Microelectron. Eng., vol. 86, pp. 1635-1637, Jul.-Sep. 2009.

[19] W. Zhu, J-P. Han, T.P. Ma, "Mobility measurement and degradation mechanisms of MOSFETs made with ultrathin high-k

dielectrics", IEEE T. Electron Dev., vol. 51, pp. 98-105, Jan. 2004.

[20] H. Wang, Y. Wang, J. Wang, C. Ye, H.B. Wang, J. Feng, B.Y. Wang, Q. Li, Y. Jiang, "Interface control and leakage current conduction mechanism in HfO_2 film prepared by pulsed laser deposition," Appl. Phys. Lett., vol. 93, pp. 202904-1-3, Nov. 2008.

[21] A. Kahraman, E. Yilmaz, S. Kaya, A. Aktag, "Effects of post deposition annealing, interface states and series resistance on electrical characteristics of HfO_2 MOS capacitors", J. Mater. Sci.: Mater. Electron., vol. 26, pp. 8277-8284, Nov. 2015.

[22] S. Kaya, E. Yilmaz, "Influences of Co-60 gamma-ray irradiation on electrical characteristics of Al_2O_3 MOS capacitors," J. Radioanal. Nucl. Ch., vol. 302, pp. 425-431, Oct. 2014.

[23] S. Kaya, E. Yilmaz, A. Kahraman, H. Karacali, "Frequency dependent gamma-ray irradiation response of Sm_2O_3 MOS capacitors," Nucl. Instrum. Meth. B,vol. 358, pp. 188-193, Sep. 2015.

[24] A. Kahraman, E. Yilmaz, A. Aktag, S. Kaya, "Evaluation of radiation sensor aspects of Er_2O_3 MOS capacitors under zero gate bias," IEEE T. Nucl. Sci., vol. 63, pp. 1284-1293, Apr. 2016.

[25] S. Maurya, "Effect of zero bias gamma ray irradiation on HfO_2 thin films," J. Mater. Sci.: Mater. Electron., vol. 27, pp. 12796-12802, Dec. 2016.

[26] A. Aktağ, E. Yilmaz, N.A.P. Mogaddam, G. Aygün, A. Cantas, R. Turan, "Ge nanocrystals embedded in SiO_2 in MOS based radiation sensors," Nucl. Instrum. Meth. B, vol. 268, pp. 3417-3420, Nov. 2010.

[27] N. Miyata, "Study of direct-contact HfO_2/Si interfaces," Materials, vol. 5, pp. 512-527, Mar. 2012.

[28] P.M. Tirmali, A.G. Khairnar, B.N. Joshi, A.M. Mahajan, "Structural and electrical characteristics of RF-sputtered HfO_2 high-k based MOS capacitors," Solid State Electron., 62, pp. 44-47, Aug. 2011.

[29] J. Robertson, "High dielectric constant oxides," Eur. Phys. J. Appl. Phys., vol. 28, pp. 265-291, Dec. 2004.

[30] A.L.S. Loke, Z-Y. Wu, R. Moallemi, C.D. Cabler, C.O. Lackey, T.T. Wee, B.A. Doybe, "Constant-Current threshold voltage extraction in HSPICE for nanoscale CMOS analog design," Advanced Micro Devices, Inc., 1-19.

[31] Silvaco. (2008, Apr.). ATHENA User's Manual. Silvaco. Santa Clara, CA. [Online]. Available: http://perso.esiee.fr/~polleuxj/Documents/athena_users.pdf

[32] C.C. Hu, "Modern Semiconductor Devices for Integrated Circuits," [Online book]. Available: https://people.eecs.berkeley.edu/~hu/Book-Chapters-and-Lecture-Slides-download.html

[33] Silvaco. (2006, Dec.) ATLAS User's Manual: Device Simulation Software. Silvaco. Santa Clara, CA. [Online]. Available: http://ridl.cfd.rit.edu/products/manuals/Silvaco/atlas_users.pdf